

DETERMINATION OF YOUNG'S MODULUS OF PZT – INFLUENCE OF CANTILEVER ORIENTATION

H. Nazeer¹, L.A. Woldering¹, L. Abelmann¹ and M.C. Elwenspoek^{1,2}

¹MESA+ Research Institute, University of Twente, P.O. Box 217, 7500 AE Enschede, The Netherlands

²FRIAS, Albert-Ludwigs University, Albertstr. 19, 79104 Freiburg, Germany

Abstract — Calculation of the resonance frequency of cantilevers fabricated from an elastically anisotropic material requires the use of an effective Young's modulus. In this paper a technique to determine the appropriate effective Young's modulus for arbitrary cantilever geometries is introduced. This technique is validated using a combined analytical and finite element simulations (FEM) approach. In addition, the effective Young's modulus of $\text{PbZr}_{0.52}\text{Ti}_{0.48}\text{O}_3$ (PZT) thin films deposited on dedicated micromachined cantilevers was investigated experimentally. The PZT films were deposited on the cantilevers by pulsed laser deposition (PLD). The change in flexural resonance frequency of the cantilevers was measured both before and after deposition of the PZT thin film. From this frequency difference we determined the Young's modulus of PZT deposited by PLD to be 103 ± 2 GPa. Even though the PZT is grown epitaxially, this value is independent of the in-plane orientation.

Keywords: Cantilever, resonance frequency, anisotropic, Young's modulus, FEM, PZT, PLD.

I – Introduction

Piezoelectric thin films are widely used in the MEMS industry for both actuation and sensing purposes [1, 2]. Many micro sized structures such as cantilevers, membranes and bridges have been employed for fabrication of the micro sensors and actuators using PZT thin films as an active material. These PZT films can be deposited by processes [3] like sol-gel, sputter deposition and pulsed laser deposition. Recently, excellent ferroelectric properties have been published about PZT deposited by PLD [4]. However, accurate determination of the mechanical properties of the PZT thin film is being hampered by the fact that up to now only mm-square areas can be deposited uniformly. Micrometer sized measurement devices provide a solution to this limitation.

The effective Young's modulus of the thin film is an important parameter to be known accurately when designing micro transducers. We devised a method to accurately determine the Young's modulus of PZT thin films by using the shift in the resonance frequency of cantilevers. An analytical relation for the determination of the effective Young's modulus of the PZT thin film was developed and experiments were conducted to measure the resonance frequency of cantilevers both before

and after the deposition of PZT thin films.

We took extra care to eliminate the errors in the determination of the effective Young's modulus of the PZT thin film. At this precision, conventional analytical expressions to calculate resonance frequencies of silicon cantilevers might not be accurate enough. 3D FEM simulations were performed to estimate the deviations between these simulations, that use anisotropic elastic properties of silicon, and the values calculated analytically for our cantilevers. The appropriate effective Young's modulus to be used in the resonance frequency calculation of our cantilevers was determined along with the corresponding errors.

II – Theory

The resonance frequency of a cantilever without PZT is calculated by using the analytical relation defined in equation (1) [5]:

$$f_n = \frac{C^2 t_s}{2\pi L^2} \sqrt{\frac{E_s^*}{12\rho}} \quad (1)$$

here f_n is the resonance frequency, C is a constant which depends on the vibration mode $C = 1.875$ for fundamental resonance frequency (f_0), E_s^* is the effective Young's modulus, ρ is the density of silicon, t_s is the thickness and L is the length of the cantilever. Calculation of the resonance frequency of silicon cantilever depends on the use of appropriate effective Young's modulus. However, single crystal silicon is elastically anisotropic. Therefore the effective Young's modulus of silicon is different for different crystal orientations. Consequently, the resonance frequencies of the cantilevers depend on their orientation with regards to the crystal lattice. For the effective Young's modulus we can either take the biaxial modulus $E/(1-\nu)$ or plate modulus $E/(1-\nu^2)$, depending on the geometry of the cantilevers. Both are however approximations. E and ν are the Young's modulus and Poisson's ratio of silicon in the particular crystal direction of silicon, see Table 1 [6]. The appropriate effective Young's modulus for our cantilevers was determined by calculating the resonance frequencies using equation (1) and by FEM simulations results for the silicon cantilevers aligned parallel to the $\langle 110 \rangle$ and $\langle 100 \rangle$ crystal directions of the silicon crystal lattice.

Full 3D finite element simulations were carried out using the COMSOL software package to verify the analytical results obtained using equation (1). To define cantilevers aligned parallel to the $\langle 110 \rangle$ orientation

Table 1: Elastic anisotropic properties of single crystal silicon.

Crystal plane {100}				
Direction	Young's modulus GPa	Poisson's ratio	$E/(1-\nu)$ GPa	$E/(1-\nu^2)$ GPa
$\langle 110 \rangle$	168.9	0.064	180.4	169.8
$\langle 100 \rangle$	130.2	0.279	180.4	141

in COMSOL, the cantilever geometry was drawn in the xy-plane with the length axis parallel to the x-axis and then rotated 45° around the z-axis. For the $\langle 100 \rangle$ cantilevers, no rotation was given to the cantilever. Standard anisotropic elastic properties of single crystal silicon as defined in the material section of the COMSOL were used for the simulations. The elastic stiffness coefficients are identical to values quoted in literature[6].

Table 2 lists the analytical calculations of resonance frequencies using equation (1) and the results of the FEM simulations of a silicon cantilever. The analytical values of the resonance frequencies calculated using a plate modulus $E/(1-\nu^2)$ agree with the FEM simulations to within 0.04 % for the $\langle 110 \rangle$ direction, and deviate by only 3 % for the $\langle 100 \rangle$ direction. The FEM results are 17 % lower when using the biaxial modulus $E/(1-\nu)$ for $\langle 100 \rangle$ aligned cantilevers. The results verify that the effective Young's modulus that we apply should be the plate modulus for the cantilever geometry which we have used in this work.

Addition of the PZT thin film on the cantilever affects the flexural rigidity and increases the mass. Both affects result in a change in the resonance frequency of the cantilever. The effective Young's modulus of the PZT thin film is calculated using the resonance frequency both before and after deposition of the PZT thin film. We developed an analytical relation for the determination of Young's modulus of PZT as described in equation (2). The equation was based on a shift of the neutral axis and on the assumptions that the cantilever has a uniform cross section and that there is small cantilever deflection [5, 7]:

$$E_f^* = \frac{1}{t_f^3} \left[6(t_s \rho_s + t_f \rho_f) B - 2E_s^* t_s^3 - 3t_f E_s^* t_s^2 - 2E_s^* t_s t_f^2 + 2 \sqrt{\frac{E_s^* t_s^2 t_f^4 + 3E_s^* t_s^3 t_f^3 + (4E_s^* t_s^4 - 3AB) t_f^2 + (3E_s^* t_s^5 - 9AB t_s) t_f + E_s^* t_s^6 - 6AB t_s^2 + 9(t_s \rho_s + t_f \rho_f)^2 B^2}{12t_s \rho_s}} \right] \quad (2)$$

where

$$A = E_s^* t_s (t_s \rho_s + t_f \rho_f) \quad \text{and} \\ B = \left(\sqrt{\frac{E_s^* t_s^3}{12t_s \rho_s}} - 0.568\pi \Delta f_o L^2 \right)^2$$

the symbols E^* , t , L and ρ are the effective Young's modulus, thickness, length and density respectively.

Subscripts s and f denotes the silicon and PZT thin film. Δf_o is the difference in the fundamental resonance frequency of the cantilever before and after the deposition of PZT. By taking this difference, any potential uncertainties in the thickness of the cantilever can be eliminated and a more accurate result is obtained [8].

 Table 2: Comparison of the fundamental resonance frequency of silicon cantilevers with length, $L = 300 \mu\text{m}$, thickness, $t_s = 3 \mu\text{m}$ and width, $w = 30 \mu\text{m}$.

Orientation	Calculated resonance frequency (Hz) for $E/(1-\nu)$	Calculated resonance frequency (Hz) for $E/(1-\nu^2)$	FEM simulation 3D, Anisotropic (Hz)
$\langle 110 \rangle$	47369	45956	45978
$\langle 100 \rangle$	47369	41878	40541

III – Fabrication

To ensure precise control of the dimensions of the cantilevers, we fabricated our $3 \mu\text{m}$ thick silicon cantilevers in a dedicated SOI/MEMS fabrication process. The fabricated cantilevers vary in length from $250 \mu\text{m}$ to $350 \mu\text{m}$ in steps of $10 \mu\text{m}$. Cantilevers were etched on the front side of the SOI wafer as detailed in Figure 1 with the following sequence. SOI wafer was selected to use the buried oxide as an etch stop (a). Application and patterning of the photoresist for defining the cantilevers (b) and (c). Deep reactive ion etching (DRIE) of the cantilevers (d). Photoresist was removed by oxygen plasma (e). Polyimide pyralin, a photoresist material, was coated as the protective layer on the front side (f).

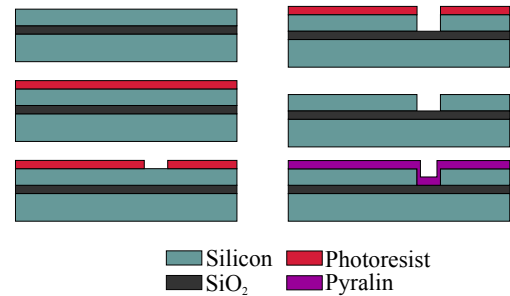


Figure 1: Fabrication process for defining cantilevers on the front side of the wafers. (a) SOI wafer, (b) application of photoresist, (c) patterning of photoresist, (d) DRIE of the silicon device layer, (e) photoresist removal, (f) application of protective layer polyimide pyralin.

Subsequently, cantilevers were released from the handle wafer by making through holes from the backside of the wafer according to the steps shown in Figure 2. Application and patterning of the photoresist for defining the holes (a) and (b). Etching of the backside of the wafer using DRIE (c). Removal of photoresist material from the top and back sides of the wafer by oxygen plasma (d). In last step the cantilevers were released by etching 500 nm of buried oxide layer using

Vapour HF (e). To measure resonance frequencies in the $\langle 110 \rangle$ and $\langle 100 \rangle$ directions, cantilevers were fabricated from a (100) single crystal silicon wafer and oriented parallel to the $\langle 110 \rangle$ and $\langle 100 \rangle$ directions of the silicon crystal lattice, see Figure 3. Buffer layers of Ytria-Stabilized Zirconia and SrRuO_3 , each 10 nm thick, were deposited by PLD on the cantilevers. These layers ensured that a high quality 100 nm PZT film could be grown epitaxially on the silicon by PLD.

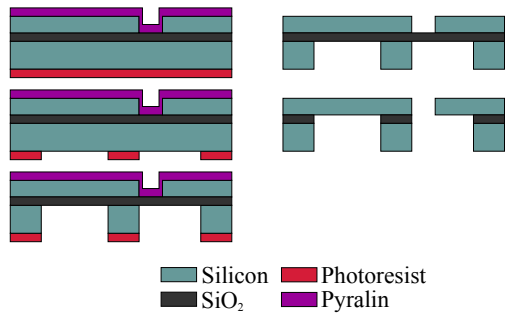


Figure 2: Fabrication steps on the backside of the wafers for releasing the cantilevers. (a) application of photoresist, (b) patterning of photoresist, (c) wafer through DRIE, (d) photoresist removal from front and back sides, (e) etching of buried oxide layer.

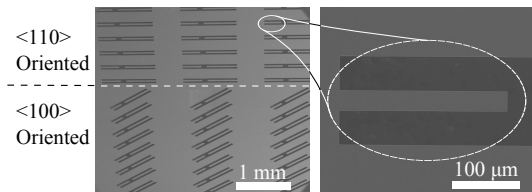


Figure 3: Scanning electron micrographs of the fabricated cantilevers. The cantilevers vary in length from 250 μm to 350 μm in steps of 10 μm . The cantilevers are aligned parallel to the $\langle 110 \rangle$ and $\langle 100 \rangle$ crystal orientations of silicon.

IV – Experimental Details

The resonance frequency of the cantilevers was measured by using a MSA-400 Micro System Analyser scanning laser-Doppler vibrometer. The measured resonance frequency before the deposition of the PZT for similar cantilevers aligned parallel to the $\langle 110 \rangle$ and $\langle 100 \rangle$ crystal orientations of silicon are shown in Figure 4. The difference of the fundamental resonance frequency for two differently oriented cantilevers can be seen clearly from the Figure 4. This difference is solely caused by the different effective Young's modulus for the two directions.

The resonance frequency of the cantilevers was again measured after the deposition of PZT. Due to the addition of the PZT thin film on the cantilevers, the resonance frequency was changed as expected, see Figure 5.

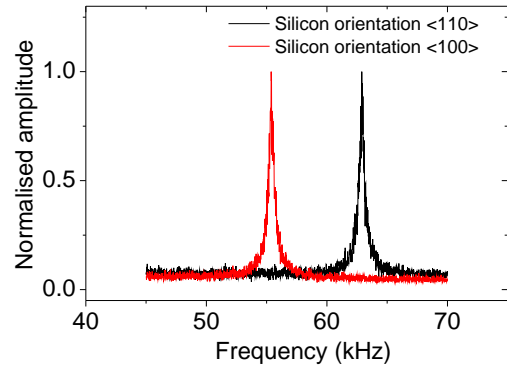


Figure 4: The difference in resonance frequency of similar cantilevers, aligned in the $\langle 110 \rangle$ and $\langle 100 \rangle$ crystal directions of the silicon crystal lattice.

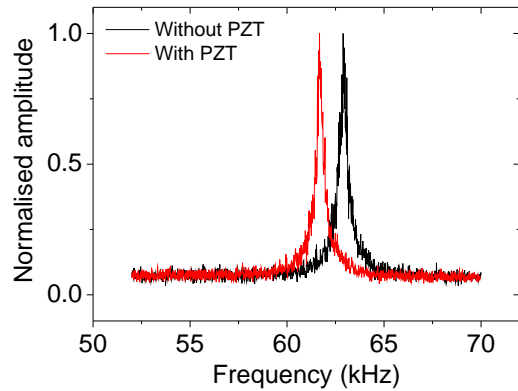


Figure 5: Measured resonance frequency before and after deposition of the PZT. The amplitude is normalised to the maximum value. The resonance frequency with PZT is lower than for the cantilevers without PZT, which is as expected.

V – Results and Discussion

Figure 6 shows that the experimentally measured resonance frequencies for the range of cantilevers length agrees well with the FEM simulations and the analytically calculated values when using the plate modulus as the effective Young's modulus of silicon.

The Young's modulus of PZT calculated by using the measured change in resonance frequency, was found to be 103 GPa with a standard error of ± 2 GPa (measured on 11 cantilevers). This value is in the same order as values quoted in literature for sol-gel [9] and sputter deposited [10] PZT. The expected change in resonance frequency, corresponding to the effective Young's modulus of PZT, was also obtained from FEM simulations. It was found that the measured change in resonance frequency is 5 to 8 % higher when compared to what is obtained from FEM simulations for different lengths of cantilevers. The origin of this discrepancy is not known

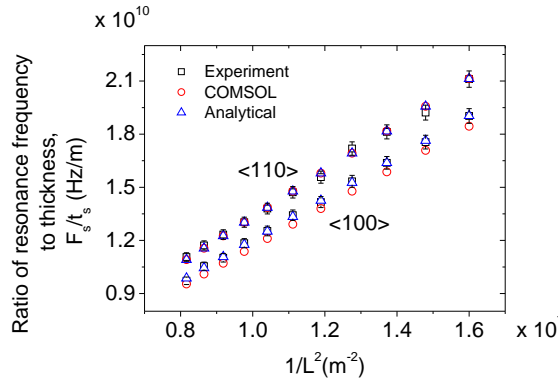


Figure 6: Analytically calculated, simulated and measured resonance frequencies for cantilevers of varying length. The cantilevers are aligned parallel to the $\langle 110 \rangle$ and $\langle 100 \rangle$ crystal directions of silicon.

to us yet.

A thorough error analysis was performed to calculate the propagation of errors in the parameters to the calculated values for the effective Young's modulus. The cumulative error found in the calculated value of the effective Young's modulus is in the order of 6 to 8 GPa for individual cantilevers. The 3 % error in the $\langle 100 \rangle$ effective Young's modulus of silicon propagates as 3.7 % error in the value of the effective Young's modulus of PZT. This suggests that a correction of the plate modulus model for the $\langle 100 \rangle$ direction might be necessary.

VI – Conclusions

In conclusion, we determined the effective Young's modulus of PZT thin films using the resonance frequency of the cantilevers both before and after the deposition of PZT. The effective Young's modulus of PZT is 103 GPa with a standard error of ± 2 GPa in both the $\langle 110 \rangle$ and $\langle 100 \rangle$ directions of silicon. We also validated by FEM simulations and experimental measurements that the plate modulus has to be used for the calculation of the effective Young's modulus of silicon for our measured cantilevers. The analytical relation for resonance frequency calculation of silicon cantilevers is very precise in the $\langle 110 \rangle$ direction. For the $\langle 100 \rangle$ direction, the deviation of analytical value compared to the simulation is only 3 %. The inaccuracy in the model however lies below the uncertainty in the measured parameters. This method of determining the appropriate effective Young's modulus is generally applicable for arbitrary cantilever geometries.

Acknowledgements

The authors gratefully acknowledge the support of the SmartMix Program (SmartPie) of the Netherlands Ministry of Economic Affairs and the Netherlands Ministry of Education, Culture and Science. The authors

also thank M.J. de Boer for etching, R.G.P. Sanders for laser Doppler vibrometer measurement, J.G.M. Sanderink for assistance with SEM, and M.D. Nguyen for depositing PZT by PLD.

References

- [1] J.R. Bronson, J.S. Pulskamp, R.G. Polcawich, C.M. Kroninger, and E.D. Wetzel. In *22nd IEEE International Conference on Micro Electro Mechanical Systems, MEMS 2009*, pages 1047–1050, Sorrento, 2009.
- [2] H.-J. Nam, Y.-S. Kim, C.S. Lee, W.-H. Jin, S.-S. Jang, I.-J. Cho, J.-U. Bu, W.B. Choi, and S.W. Choi. *Sensors and Actuators A: Physical*, 134(2):329–333, 2007.
- [3] Y.C. Zhou, Z.Y. Yang, and X.J. Zheng. *Surface and Coatings Technology*, 162(2-3):202–211, 2003.
- [4] M. Dekkers, M.D. Nguyen, R. Steenwelle, P.M. te Riele, D.H.A. Blank, and G. Rijnders. *Applied Physics Letters*, 95(1):012902–012902–3, 2009.
- [5] E. Volterra and E.C. Zachmanoglou. *Dynamics of vibrations*. CE Merrill Books, 1965.
- [6] W.A. Brantley. *Journal of Applied Physics*, 44(1):534–535, 1973.
- [7] J.M. Gere. *Mechanics of Materials*. 6th. Toronto, Canada: Thomson-Engineering, 2006.
- [8] J.-A. Schweitz. *Journal of Micromechanics and Microengineering*, 1(1):10–15, 1991.
- [9] B. Piekarski, D. DeVoe, M. Dubey, R. Kaul, and J. Conrad. *Sensors and Actuators A: Physical*, 91(3):313–320, July 2001.
- [10] T.H. Fang, S.R. Jian, et al. *Journal of Physics: Condensed Matter*, 15:5253–5259, 2003.